ChemPubSoc Europe

DOI: 10.1002/cbic.201900024

CHEMBIOCHEM Full Papers

VIP *Very Important Paper*

The Structural Determinants Accounting for the Broad Substrate Specificity of the Quorum Quenching Lactonase GcL

Celine Bergonzi, Michael Schwab, Tanushree Naik, and Mikael Elias*[a]

Quorum quenching lactonases are enzymes capable of hydrolyzing lactones, including *N*-acyl homoserine lactones (AHLs). AHLs are molecules known as signals in bacterial communication dubbed quorum sensing. Bacterial signal disruption by lactonases was previously reported to inhibit behavior regulated by quorum sensing, such as the expression of virulence factors and the formation of biofilms. Herein, we report the enzymatic and structural characterization of a novel lactonase representative from the metallo-β-lactamase superfamily, dubbed GcL. GcL is a broad spectrum and highly proficient lactonase, with k_{cat}/K_M values in the range of 10^4 to 10^6 $M^{-1}s^{-1}$. Analysis of free GcL structures and in complex with AHL substrates of different acyl chain length, namely, C4-AHL and 3-oxo-C12-AHL, allowed their respective binding modes to be elucidated. Structures reveal three subsites in the binding crevice: 1) the small subsite where chemistry is performed on the lactone ring; 2) a hydrophobic ring that accommodates the amide group of AHLs and small acyl chains; and 3) the outer, hydrophilic subsite that extends to the protein surface. Unexpectedly, the absence of structural accommodation for long substrate acyl chains seems to relate to the broad substrate specificity of the enzyme.

Introduction

Quorum sensing (QS) is a communication system used by numerous microorganisms to coordinate various behaviors. QS is based on small molecules produced and secreted by microorganisms, such as *N*-acyl-L-homoserine lactone (AHLs).[1] The structure of AHLs can vary significantly, mainly by the length of the acyl chain, as well as substitutions on it. Different chemical structures confer signal specificity.[2,3] These molecules can be sensed and their signal integrated to coordinate gene expression in response to cell density. AHL-based bacterial QS was shown to regulate the expression of gene patterns, including genes involved in virulence and biofilm production.[4] Numerous enzymes, named quorum quenching (QQ) enzymes, are naturally capable of modifying or degrading QS signals.[5] These enzymes are capable of disrupting microbial signaling, and were reported to inhibit biofilm formation and virulence both in vitro and in vivo.[6–10] Therefore, these enzymes may be useful in various fields to control microbes, from biofouling prevention to therapeutics or combination therapy with antibiotics.[6,7,11]

Among those enzymes, lactonases (EC 3.1.1.81) are capable of hydrolyzing the lactone ring of AHLs. Lactonases were identified in a wide variety of organisms, for example, in archaea, fungi, and mammals.[12] Lactonases were mainly identified and characterized from three protein superfamilies; all were metalloenzymes.[12] The phosphotriesterase-like lactonases (PLLs) exhibit an $(\alpha/\beta)_8$ fold and are found in archaea and bacteria. PLL representatives were found to hydrolyze δ-lactones, γ-lactones, and AHLs and showed substrate preference for long acyl chain AHLs.[13–16] A second family of lactonases are the paraoxonases (PONs), primarily isolated from mammals, exhibit a six-bladed β-propeller fold.[17–19] PONs were shown to hydrolyze δ-lactones, γ-lactones, and AHLs.[20]

A third family of lactonases are the metallo-β-lactamase-like lactonases (MLLs), the first lactonase family to be discovered, and exemplified by the first isolated and studied representative: AiiA from *Bacillus thuringiensis*.[9] Other representatives have been studied, such as AiiB,[21] AidC,[22] MomL,[23] or AaL.[24] MLLs possess a conserved dinuclear metal binding motif, HXHXDH, involved in the binding of two metal cations and exhibit an αβ/βα fold. Interestingly, kinetic characterization studies on MLLs suggest that they all exhibit a broad specificity spectrum,[21,25–27] which is in contrast to the observed preference of PLLs for long-chain AHLs. Despite this shared substrate preference, kinetic studies reveal differences: K_M values vary dramatically from about the 1 mM range for some enzymes (e.g., AiiA, AiiB[21,27]) to about 1 μM range for others (e.g., AidC, AaL[22,24]).

Intriguingly, structural studies on AiiA,[27–29] AiiB from *Agrobacterium tumefaciens*,[21] AidC from *Chryseobacterium* sp. strain StRB126,[22] and AaL from *Alicyclobacter acidoterrestris*[24] reveal differences in their respective active sites. For example, AidC exhibits a kinked α helix, forming part of a closed pocket,[22]

[a] C. Bergonzi, M. Schwab, T. Naik, Prof. Dr. M. Elias
Biochemistry, Molecular Biology and Biophysics Department and BioTechnology Institute, University of Minnesota
Saint Paul, MN 55108 (USA)
E-mail: mhelias@umn.edu

Supporting information and the ORCID identification numbers for the authors of this article can be found under https://doi.org/10.1002/cbic.201900024.

This article is part of the young researchers' issue ChemBioTalents. To view the complete issue, visit http://chembiochem.org/chembiotalents

whereas AaL shows a hydrophobic patch;[24] both features are related to the lower K_M values of these enzymes for AHLs. Nevertheless, a molecular description of the interaction of lactonases with AHL substrates of different sizes and an explanation for the absence of substrate preference of MLLs are missing.

GcL (WP_017434252.1) is a lactonase isolated from the thermophilic bacteria *Parageobacillus caldoxylosilyticus*. GcL is a rare thermophilic representative within MLLs, with a half-life of (152.5 ± 10) min at 75 °C.[25] Herein, we show that GcL is a proficient lactonase, which makes it a potent inhibitor of biofilm formation for the pathogen *Acinetobacter baumannii* that uses C6-AHL for signaling.[30,31] Because structural variations of AHLs confer signal specificity, it is critical to elucidate substrate preferences. We determined that GcL was a broad spectrum lactonase, with k_{cat}/K_M values in the range of 10^4 to 10^6 $M^{-1}s^{-1}$, and very low K_M values (0.5–20 μM). Broad lactonase activity may be a desirable property to control microbial signaling. Additionally, we provide herein a unique collection of structures: the structure of free GcL and in complex with AHL substrates of different acyl chain lengths, namely, C4-AHL and 3-oxo-C12-AHL. These structures allowed us to determine the substrate binding modes of these very different AHLs, and to identify three different subsites involved in the binding of substrates. Unexpectedly, the outer part of the active site is not hydrophobic and overall the active-site crevice is too short to fully accommodate the longer AHLs; thus resulting in the acyl tail of the substrate trailing outside of the enzyme. This binding mode is in contrast to the dedicated, hydrophobic channel fully accommodating the aliphatic chain previously observed in PLLs with a preference for long-chain AHLs.

Results and Discussion

Sequence analysis

The GcL protein sequence was aligned with sequences of MLL representatives with known structures by using the MUSCLE program[32] (Figure S1 in the Supporting Information). GcL is very close to AaL (85.5% sequence identity), whereas it shares only 28% sequence identity with both AidC and AiiA. These enzymes possess the characteristic HXHXDH motif, as well as the two other residues (H and D) involved in metal-cation coordination. Other residues lining the active site do not show significant conservation, with the exception of Y223 (Figure S1). Indeed, Y223 is conserved in all enzymatically and structurally characterized MLLs, with the exception of AidC,[22] in which it is substituted by a His. Interestingly, this residue is also present in PLLs.[12,33,34]

GcL as a highly proficient, broad-spectrum lactonase

The catalytic parameters of GcL were evaluated for a broad range of lactones, including AHLs, 3-oxo-AHLs, γ-lactones, ε-lactones, δ-lactones, and the whiskey lactone (Figures 1 and S2, Table 1). We show that GcL is highly proficient against AHLs with both short and long acyl chains, exhibiting catalytic efficiencies ranging from 10^4 to 10^6 $M^{-1}s^{-1}$. In addition to AHLs, GcL is active against γ-, δ-, ε-, and whiskey lactone, with k_{cat}/K_M values ranging from 10^5 to 10^7 $M^{-1}s^{-1}$. Notably, γ-butyrolactone derivatives are inducers for *Streptomyces* sp. and *Rhodococcus* sp.[35,36] The slowest tested substrate is C4-AHL, with a catalytic efficiency of 8.3×10^4 $M^{-1}s^{-1}$, whereas the best substrate is 3-oxo-C8 AHL ($k_{cat}/K_M = 4.3\times10^6$ $M^{-1}s^{-1}$). Kinetic data reveals that GcL exhibits unusually low K_M values for a large majority of the tested substrates (0.84–24.7 μM, with the exception of C4 AHL), compared with those values of other known lactonases. Notably, the limited dynamic range of the pH indicator based assay used could limit the observation of lower K_M values. The observed K_M value for GcL is in contrast to values observed for other MLL lactonases, such as AiiA and AiiB ($K_M \approx 1600$–5600 μM[21,27]), and other classes of lactonases (e.g., PLLs and PONs; $K_M \approx 50$–500 μM[13,15,20,28]). Yet, these low K_M values are similar to those observed for AidC and AaL.[22,24] The K_M values of lactonases are important to consider in light of the concentration thresholds for QS activation, which are reported to be

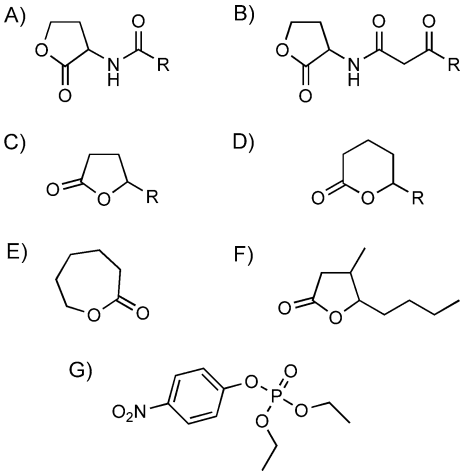

Figure 1. Substrates tested in this study. A) Acyl homoserine lactones, B) 3-oxoacyl homoserine lactones, C) γ-lactones, D) δ-lactones, E) ε-caprolactone, F) whiskey lactone, and G) Paraoxon-ethyl.

Mikael Elias received his B.S. (2004) and M.S. (2006) degrees from the Université de Lorraine (France) and his Ph.D. degree (2009) from the Université Aix–Marseille (France). He joined the Weizmann Institute of Science (Rehovot, Israel) as a FEBS postdoctoral fellow (2009), where he worked as a visiting scientist and later (2011) as a Marie Curie Fellow. Since the fall of 2014, he has been Assistant Professor at the University of Minnesota (USA). His research lies at the interface of biology and chemistry. Foremost, he is interested in an atomic-level understanding of the molecular determinants underlining molecular recognition, promiscuity, and ultrahigh specificity.

Table 1. Enzymatic characterization of GcL enzymes. Unless otherwise specified, racemic substrates have been used. The standard deviation values for each parameter are given and data are taken from ref. [25].

Substrate[a]	k_{cat} [s^{-1}]	K_M [μM]	k_{cat}/K_M [s^{-1} M^{-1}]
C4-AHL (l)*	19.06 ± 1.51	229 ± 57	(8.3 ± 2.2) × 10^4
C6-AHL (l)*	8.95 ± 0.48	7.97 ± 1.89	(1.1 ± 0.3) × 10^6
C8-AHL (l)	1.29 ± 0.04	3.12 ± 0.75	(4.1 ± 1.0) × 10^5
C10-AHL (l)*	5.48 ± 0.37	1.45 ± 0.47	(3.8 ± 1.3) × 10^6
3-oxo-C8-AHL (l)*	9.48 ± 0.35	2.19 ± 0.37	(4.3 ± 0.8) × 10^6
γ-butyrolactone	2.49 ± 0.07	10.1 ± 1.92	(2.5 ± 0.5) × 10^5
γ-heptalactone	1.77 ± 0.06	2.01 ± 0.71	(8.8 ± 3.1) × 10^5
γ-nonalactone	20.5 ± 6.9	15.3 ± 2.23	(1.3 ± 0.2) × 10^6
γ-decanolactone	2.69 ± 0.11	7.14 ± 1.03	(3.8 ± 0.6) × 10^5
δ-valerolactone	1.24 ± 0.04	6.11 ± 1.37	(2.0 ± 0.5) × 10^5
δ-octanolactone	12.58 ± 0.85	18.3 ± 7.02	(6.9 ± 2.7) × 10^5
δ-nonalactone	2.01 ± 0.14	8.05 ± 2.5	(2.5 ± 0.8) × 10^5
δ-decalactone	4.1 ± 0.18	3.13 ± 0.9	(1.3 ± 0.4) × 10^6
ε-caprolactone	10.81 ± 0.57	24.7 ± 5.43	(4.4 ± 0.9) × 10^5
ε-decalactone	1.09 ± 0.03	1.04 ± 0.24	(1.1 ± 0.2) × 10^5
whiskey lactone	1.00 ± 0.35	0.84 ± 0.18	(1.2 ± 0.1) × 10^7
Paraoxon-ethyl	n.d.[b]	n.d.[b]	(3.1 ± 0.2) × 10^1

[a] Structures are given in Figure S1. [b] n.d.: the kinetics data do not fit the Michaelis–Menten equation due to a catalytic rate that is too high or too low.

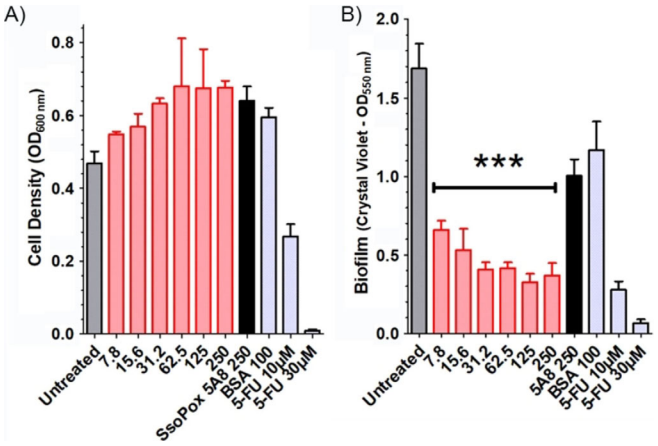

Figure 2. Effect of GcL on A) cell density and B) biofilm formation of *A. baumannii*. The biofilm was quantified by means of crystal violet staining ($OD_{550\,nm}$). The cell density is quantified as $OD_{600\,nm}$. The biofilm was quantified with untreated cultures (dark-gray bars); various doses of GcL (μg mL^{-1}; red bars); and negative controls, such as the inactive mutant of the lactonase SsoPox (5A8; black bar) and bovine serum albumin (BSA; light-gray bars). The positive control (quorum sensing inhibitor (QSI) 5-fluorouracil (5-FU)) is shown as light-gray bars. GcL, SsoPox 5A8, and BSA concentrations are shown in μg mL^{-1}. Data shown are an average of three independent experiments with two technical replicates each ($n = 6$); error bars represent the standard deviation. The Student t-test (unpaired, two-tailed) results are shown (A) between data for the biofilm formed with different doses of GcL and data for the biofilm formed in presence of the inactive lactonase 5A8.

in the range of about 5 nM.[37–41] Additionally, we tested the ability of GcL to degrade the insecticide derivative Paraoxon, and determined that it was capable of degrading it, albeit with slow rates. This promiscuous activity of GcL is consistent with previous observations in other lactonases, such as AaL,[24] and the PLL family, such as VmoLac[13] and SsoPox,[14] which exhibit higher phosphotriesterase activities. The promiscuous ability of lactonases to degrade the phosphotriester Paraoxon is consistent with the previously proposed evolutionary link between lactonases and phosphotriesterase.[12,42] In fact, lactonases were suggested to be the progenitors of the insecticide-degrading enzyme PTE,[42] which emerged during the last 70 years to degrade synthetic insecticides, the organophosphates.

GcL as a QQ lactonase

We have evaluated the ability of the lactonase GcL to inhibit biofilm formation of *A. baumannii*; a human pathogen known to produce and utilize acyl homoserine lactone. QQ lactonases are known to disrupt AHL-based signaling and inhibit bacterial behavior that depends on signaling, such as biofilm formation,[38,43] and even disrupt existing biofilms.[39] Herein, we show that GcL can inhibit the formation of biofilms of *A. baumannii* in a dose-dependent manner. Biofilm inhibition is up to fivefold with reference to untreated cultures, and about threefold compared with an inactive lactone control (inactive mutant SsoPox 5A8, obtained previously;[14,44] Figure 2). Interestingly, and as previously observed for the lactonases SsoPox[6,10] and AaL,[24] GcL has no negative effects on growth and exhibits similar growth levels to those of the controls performed with BSA and 5A8 mutant. This observation is in contrast to the use of the QSI 5-FU,[45] which inhibits both growth and biofilm formation. In fact, GcL treatment may lead to a slight growth stimulation. However, because this is concomitant with biofilm inhibition, it may simply relate to a different partitioning of the cells in both planktonic and biofilm states.

Crystal structure of GcL

The monomer of GcL is roughly globular with overall dimensions of 58 × 43 × 44 Å and shows a long protruding loop (Figure S3 A–C). This loop is involved in homodimerization (Figure S3 A). The dimer shows overall dimensions of approximately 85 × 43 × 44 Å. As expected, GcL exhibits an αβ/βα sandwich fold, typical of the metallo-β-lactamase superfamily, and similar to that of other MLLs (AiiA,[29] AiiB,[21] AidC,[22] and AaL[24]).

The overall structure of GcL is very similar to those of AaL, with a root-mean-square deviation (rmsd) of 0.42 Å (over 275 α-carbon atoms; Figure S4 C), and AiiB (0.89 Å over 273 α-carbon atoms; Figure S4 B). However, the structural differences are much greater between GcL and AiiA, with an rmsd of 1.22 Å (over 180 α-carbon atoms), including the noticeable absence of external loop 1 in AiiA (Figure S4 A). The finding that GcL, isolated from a thermophilic bacterium, and contrary to AiiA,[29] is organized as a homodimer is consistent with previous work on thermophilic proteins; thus highlighting a trend for higher levels of oligomerization in these proteins.[46] The dimer is characterized by a strong interaction of the protruding loop (Ala34 to Gln42) from both monomers. The dimer interface involves 32 residues in each monomer. The interface is mostly hydrophobic and engages 12 hydrogen bonds. The interface surface between dimers is 1178.9 $Å^2$; a similar value

to those of other dimeric MLL structures, such as AaL, AiiB, and AidC (1125.7, 1089.1, and 1015.4 Å^2, respectively).

Hetero-bimetallic active site of GcL

The GcL active site (Figure S3 D) is organized around two metals cations coordinated by five histidine residues (118, 120, 123, 198, and 266) and two aspartic acid residues (122 and 220). The α-metal cation is coordinated by His118, His120, His198, and Asp220. The β-metal cation interacts with His123, His266, Asp122, and Asp220. The putative catalytic water molecule bridges the two metal cations.

The chemical nature of the metals was investigated by using X-ray anomalous and anomalous data collection at higher and lower energies than that of the Co K edge (Table S1). Above the Co K edge, two strong anomalous peaks are present in the active site, which indicates that the active site may be occupied by cobalt cations, but not by other common metal cations identified in similar enzymes, such as zinc (Zn K edge is 9.6586 keV) or nickel (Ni K edge is 8.3328 keV; Figure S5). The second dataset collected at a lower energy than that of the Co K edge reveals only one peak; this unambiguously determines metal α as a cobalt cation (Figure S5). The second peak corresponds to a different metal cation with a lower excitation energy, which is likely to be an iron cation.

Although this result contrasts with some known enzymes from the MLL family, which were described to possess two zinc cations in their active site,[22,27,29] a hetero-binuclear iron/cobalt active site was previously observed in the lactonase SsoPox, for which the presence of an iron cation was associated with the lower pK_a of the Fe/H_2O couple to that of values with other cations.[34] Two cobalt cations were also observed in the lactonase AaL.[24] Moreover, the presence of a cobalt cation in the active site of GcL is consistent with our use of $CoCl_2$ during the protein production steps. For these reasons, a hetero-binuclear cobalt/iron was modeled in the active site of GcL.

Binding mode of the short lactone C4-AHL (L enantiomer)

Interestingly, GcL crystals soaked with C4-AHL belong to a different space group than that of the crystals of the free enzyme (*R*3, as opposed to *C*2 space groups; Table 2). Inspection of the electron density maps at 2.35 Å resolution unambiguously reveals the presence of a C4-AHL substrate bound to the bimetallic active site (Figure S6 A and B). This structure represents the second complex of a MLL with a short AHL chain, based on recent work on the lactonase AaL.[24] Other structures with hydrolytic products were solved for AiiA.[27,47]

The lactone ring of the C4-AHL molecule sits on the bimetallic active site (Figure 3 A and B). The carbonyl oxygen interacts with the α-cobalt (2.6 Å) and the hydroxyl group of Tyr223 (3.0 Å). The ester oxygen of the lactone ring interacts with the β-iron (2.2 Å). The two metal cations are bridged by the putative catalytic water (α-cobalt: 2.1 Å; β-iron: 2.3 Å). The catalytic water is located 2.5 Å away from the electrophilic carbon of the lactone ring; this binding configuration is compatible with nucleophilic attack of the bridging water molecule, as previously proposed.[24,27,34]

Table 2. Data collection and refinement statistics of GcL structures.

	Free	C4-AHL bound	3-oxo-C12-AHL bound
PDB ID	6N9I	6N9Q	6N9R
resolution [Å]	1.6	2.35	1.75
diffraction source	APS Argonne 23ID-B	APS Argonne 23ID-B	APS Argonne 23ID-D
wavelength [Å]	1.03323	1.033200	1.03333
detector	MAR CCD	EIGER 16M	PILATUS
rotation range per image [°]	0.5	0.2	0.2
total rotation range [°]	200	250	220
space group	*C*2	*R*3	*C*2
Unit-cell parameters			
[Å]	$a=145.42$, $b=108.68$, $c=78.74$	$a=108.02$, $b=108.02$, $c=222.14$	$a=145.01$, $b=108.59$, $c=78.60$
[°]	$\alpha=\gamma=90.000$, $\beta=115.845$	$\alpha=\beta=90.000$, $\gamma=120.000$	$\alpha=\gamma=90.000$, $\beta=115.747$
resolution range [Å]	1.6 (1.7–1.6)	2.35 (2.45–2.35)	1.75 (1.85–1.75)
no. reflns (last bin)	602 221 (99 530)	292 862 (33 693)	436 367 (68 612)
no. unique reflns (last bin)	144 425 (23 974)	39 818 (4637)	109 519 (16 825)
completeness [%] (last bin)	99.6 (99.7)	98.9 (98.5)	99.2 (99.5)
redundancy	4.17 (4.15)	7.35 (7.27)	3.98 (4.07)
$\langle I/\sigma(I)\rangle$	26.50 (3.1)	12.41 (4.30)	15.21 (3.32)
R_{meas} [%]	3.3 (64.5)	11.9 (54.8)	5.9 (48.0)
$CC_{1/2}$	100 (99.4)	99.5 (89.8)	99.9 (94.7)
Refinement statistics			
R_{free}/R_{work}	18.86/14.45	21.09/16.84	20.61/23.36
no. total model atoms	7065	6942	4514
Ramachandran favored [%]	96.23	95.64	96.47
Ramachandran outliers [%]	0.12	0.00	0.00
generously allowed rotamers [%]	2.14	2.24	2.23
RMSD from ideal			
bond lengths [Å]	0.0258	0.019	0.016
bond angles [°]	2.3575	1.973	1.772

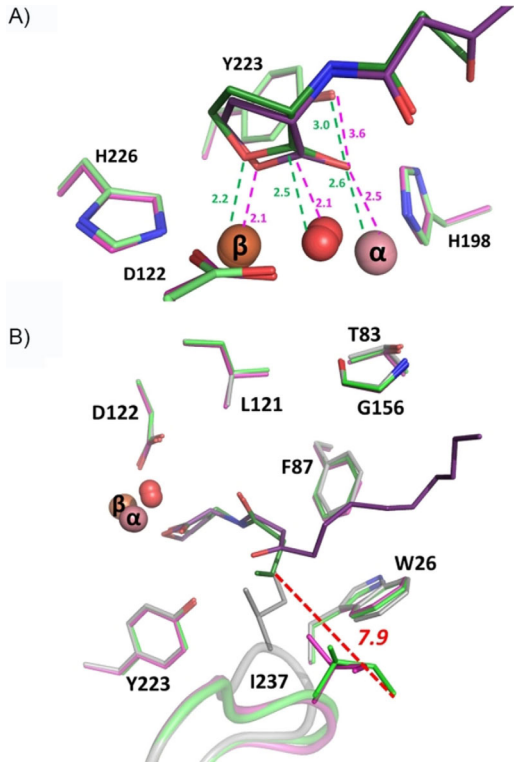

Figure 3. GcL complex with C4 and 3-oxo-C12 AHL. A) C4 and 3-oxo-C12 AHL active-site binding mode. Superposition of the C4-AHL-bound structure (light-green sticks (protein) and dark-green sticks (C4-AHL)) and 3-oxo-C12 AHL (purple sticks (protein) and dark-purple sticks (3-oxo-C12 AHL)) onto the hetero-bimetallic active site, consisting of a cobalt α-cation (pink sphere) and an iron β-cation (orange sphere). The α- and β-cation metals are bridged by the catalytic water molecule (red sphere). The interactions between C4-AHL and 3-oxo-C12 AHL and the active site are showed as green and pink dashes, respectively. Distances are indicated in Å. B) Superposition of the free GcL structure (gray sticks and cartoon) and the C4-AHL (green sticks and cartoon; substrate in dark-green sticks) and 3-oxo-C12-AHL (pink sticks and cartoon; substrate in dark-purple sticks) bound structures. The important relocation of the Ile237 loop (7.9 Å) between the free and C4-AHL bound structures is shown as red dashes.

The N-alkyl chain of C4-AHL interacts with the hydrophobic patch formed by Trp26, Phe87, and Ile237 (Figure 3B). Specifically, the N-alkyl chain is kinked in the direction of Ile237 (Figure 3B). In fact, this hydrophobic patch, previously described in the close homologue AaL,[24] has no equivalent in other MLLs. Its presence has been proposed to be related to the low K_M values observed in AaL, and this is consistent with the structure and kinetic parameters of GcL. Additionally, bound C4-AHL also interacts with two Met (20 and 22), Phe48, Tyr223, Leu121, and Ala157 (Figure 4).

Binding mode of the long, aliphatic lactone 3-oxo-C12-AHL (L enantiomer)

The crystal soaking strategy (see the Experimental Section) allowed us to solve the structure of GcL at 1.75 Å resolution. Inspection of the electron density maps unambiguously reveals the binding of the long, aliphatic lactone substrate in the active site (Figure S6C and D). The binding mode of the lactone ring onto the bimetallic active site is very similar to that observed for the shorter lactone C4-AHL (Figure 3A). Indeed, the ester oxygen atom of the lactone ring interacts with the β-iron (2.1 Å) and Tyr223 (3.6 Å), and the carbonyl oxygen atom is located 2.5 Å from the α-cation cobalt. The bridging, putatively catalytic water molecule is positioned 2.1 Å away from the electrophilic carbon of the lactone ring. The high similarity in binding of the lactone rings of both substrate is consistent with the broad specificity of GcL.

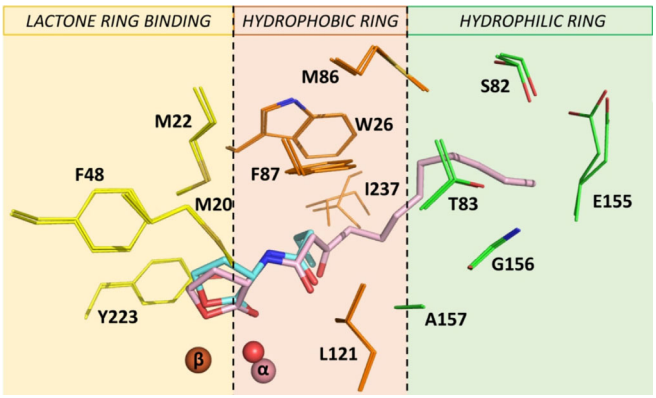

Figure 4. Superposition of the GcL structures bound to C4- (light-blue sticks) and 3-oxo-C12- AHL (light-pink sticks). The GcL active site can be divided into three subsites: the first subsite (residues in yellow lines) represents residues overhanging the binuclear center and positioning of the lactone ring, the second subsite (amino acids in orange lines) is composed of a hydrophobic ring that accommodates the amide group and short acyl chains of AHL substrates, and the third subsite (residues in green lines) is a hydrophilic ring open to the solvent.

The N-alkyl chain of the 3-oxo-C12 AHL is surrounded by three methionine residues (20, 22, 86), two phenylalanine residues (48, 87), Trp26, Ser82, Thr83, Leu121, Asp122, Gln153, Glu 155, Gly156, Ala157, Tyr223, and Ile237 (Figure 4). Notably, the N-alkyl chain interacts with the previously described hydrophobic patch (i.e., Trp26, Phe87, and Ile237), but, contrary to the C4-AHL configuration, it is not pointing towards it (Figures 3C and 4). This difference in binding modes might be caused by the lower configurational flexibility of the substrate chain in this area due to the presence of a ketone group.

Structural changes in the GcL structure induced by AHL substrate binding

The binding of AHLs to the active site of GcL results in significant rearrangement of the binding cleft. The active-site loop harboring Ile237 undergoes significant relocation upon AHL binding (Figure 3B). In the free structure, the Ile237 side chain points inwards, which results in a closed conformation of the active site. In the presence of the C4- and 3-oxo-C12-AHLs, the 237 loop undergoes a conformational change, and the Ile237 side chain points outwards, which opens up the binding cleft (Figure 3B). The magnitude of the movement is important because the side-chain atoms of Ile237 are distant by as much as 7.9 and 7.3 Å, upon comparing the free structure with the C4- and 3-oxo-C12-AHL bound structures, respectively. This obser-

vation suggests that Ile237 is a key residue for AHL binding, and might act as a gate to the active site of GcL.

Three subsites revealed by AHL binding-mode analysis

We provide, for the first time, crystal structures of a lactonase in complex with AHLs of different chain lengths. Structural analysis of the three obtained structures of GcL—free, bound to C4-AHL, and bound to 3-oxo-C12-AHL—reveals the existence of three subsites in the active site of the lactonase GcL (Figure 4).

The three subsites are identified as follows: 1) A small subsite, which is hydrophobic and overhanging the bimetallic active-site center, involved in the accommodation of the lactone cycle, and composed of residues Met20, Met22, Phe48, and Tyr223. 2) The second subsite, which is a hydrophobic ring including Trp26, Met86, Phe87, Leu121, and Ile237, accommodates the amide group and short N-acyl chains of AHLs (i.e., the chain of the C4-AHL molecule; Figure 4). The previously identified hydrophobic patch in the lactonase AaL,[24] Trp26, Phe87, and Ile237, is a ring that may explain the low K_M values for AHL substrates of GcL. 3) Lastly, a third subsite, which involves hydrophilic ring opening to the protein surface, composed of Ser82, Thr83, Glu155, Gly156, and Ala157, accommodates the longer acyl chain of AHLs (i.e., 3-oxo-C12-AHL; Figure 4).

The presence of hydrophilic residues is surprising, given the hydrophobic nature of long-chain AHL molecules. The active-site crevice is too short to fully accommodate the length of the N-acyl chain of 3-oxo-C12-AHL (Figure 5 A). This is in sharp

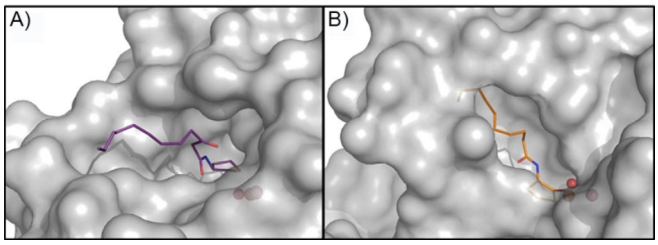

Figure 5. A comparison of active-site clefts of A) GcL and B) SsoPox. A) The structure of GcL bound to a 3-oxo-C12-AHL (dark-purple sticks) shows a large opening of the cavity, leading to the bimetallic active site. The distal part of the aliphatic chain is largely exposed to solvent. B) The structure of SsoPox bound to C10-HTL (orange sticks). SsoPox presents a deep channel, leading to the bimetallic active site. The substrate is fully accommodated in the hydrophobic channel. Metal cations and the bridging water molecules are shown as spheres.

contrast with previous structures of lactonases solved in complex with C10 homocysteine thiolactone and with 3-oxo-C12-AHL.[13,34] Indeed, in these lactonases, a hydrophobic channel isolates the hydrophobic N-acyl chain from the solvent; a structural feature associated with the preference of PLLs for longer AHL substrates[34] (Figure 5 B). Conversely, in GcL, the crevice is short, the outer ring of residues is hydrophilic, and the N-acyl chain is exposed to solvent (Figure 5 A). The absence of specific hydrophobic interactions observed in GcL seem to result in its very broad substrate specificity for hydrolysis of AHLs with short or long N-acyl chains with nearly identical parameters.

Conclusion

GcL, isolated from *P. caldoxylosilyticus*, is a thermophilic lactonase from the MLL family. We have demonstrated herein that GcL was a QQ lactonase that could significantly inhibit the formation of biofilms of *A. baumannii* in a dose-dependent manner.

GcL is a very broad spectrum lactonase, capable of hydrolyzing short and long AHLs with high catalytic efficiency ($k_{cat}/K_M \approx 10^4$–10^6 $M^{-1}s^{-1}$). This observed broad substrate specificity appears to be a common feature of MLLs because it has been observed for MomL,[23] AidC,[22] AaL,[24] or AiiA.[48] Moreover, GcL shows low K_M values for all tested lactone substrates (0.67–229 μM). K_M values might be an important parameter in the biological roles of QQ lactonases because the reported QS activation thresholds seem to be in the range of about 5 nM.[40,41] Notably, the GcL substrate specificity extends to δ-, γ-, and ε-lactones. Interestingly, some γ-lactones are used as QS molecules in *Streptomyces* and *Rhodococcus*.[35,49]

The resolution of GcL structures, in complex with short and long AHL substrates, shed light on the binding modes for different AHL substrates in lactonases. Specifically, we showed that the lactone rings of both AHLs (C4- and 3-oxo-C12-AHL) bound similarly to the bimetallic active site of the enzyme, and were ideally positioned for nucleophilic attack from the bridging water molecule. Structural data revealed the reorganization of the active-site loop harboring Ile237 upon ligand binding; this loop was locked in a closed conformation if the enzyme was free, whereas it pointed outwards if an AHL molecule was bound.

Structures also revealed that the GcL active site was organized into three subsites: one that was hydrophobic, overhanging the binuclear center, to position the lactone ring; a second that was composed of a hydrophobic ring to accommodate the amide group and short acyl chains of AHL substrates, and possibly determining the low K_M values of GcL for lactone substrates; and a third composed of an outer hydrophilic ring opening to the solvent. The last subsite was a surprise: indeed, previously known structures of lactonases in complex with long-chain AHLs revealed channels fully accommodating the hydrophobic substrates, which conferred a substrate preference for long-chain AHLs to these enzymes. Conversely, GcL structures revealed the absence of such a structural feature; thus suggesting that this absence was the main determinant for the broad substrate specificity of GcL.

Experimental Section

Sequence blast: The FASTA sequence of the first structurally characterized MLL enzyme, AiiA from the organism *B. thuringiensis*, was blasted against the nonredundant protein sequences database. We identified the protein GcL (WP_017434252.1), which was isolated from the thermophilic organism *P. caldoxylosilyticus*. GcL exhibited

a molecular weight of 32.4 kDa and contained 282 amino acids. GcL alignment with other representatives of the MLLs was perform by using the software MUSCLE[32] in the MEGA software suite[50] (Figure S1).

Cloning, expression, and purification of the protein GcL: The protein was produced in *Escherichia coli* strain BL21(DE3)-pGro7/GroEL strain (TaKaRa). A StrepTag (WSHPQFEK) was added to the sequence, along with a TEV sequence (ENLYFQS). The protein was produced at 37 °C in the autoinducer medium ZYP (2 L; 100 mg mL^{-1} ampicillin and 34 mg mL^{-1} chloramphenicol). Once the $OD_{600\,nm}$ reached the exponential growth phase, the culture was induced with 2 mM $CoCl_2$ and 0.2% L-arabinose. The induction process temperature was 18 °C overnight. Cells were harvested through centrifugation and the pelleted cells were resuspended in lysis buffer (150 mM NaCl, 50 mM HEPES pH 8.0, 0.2 mM $CoCl_2$, 0.1 mM PMSF, and 25 mg mL^{-1} lysozyme) and left in ice for 30 min. Then, cells were sonicated in three steps over 30 s (1 pulse-on; 2 pulse-off) at amplitude 45 (Q700 Sonicator, Qsonica, USA). After sonication, the supernatant lysate was loaded on a Strep Trap HP chromatography column (GE Healthcare) in PTE buffer (50 mM HEPES pH 8.0, 150 mM NaCl and 0.2 mM $CoCl_2$) at room temperature. The StrepTag was cleaved by using the tobacco etch virus (TEV) protease (reaction 1:20, *w/w*) for 20 h at 4 °C. Finally, the concentrated sample was loaded on a size-exclusion column (Superdex 75 16/60, GE Healthcare) to obtain a pure protein. The protein identity and purity were controlled by means of Coomassie-stained SDS-PAGE.

Kinetic measurements: The determination of GcL catalytic efficiency was performed by using a microplate reader (Synergy HTX, BioTek, USA) and the software Gen5.1 over a range of substrates (Figure 1). The reactions were operated in a 96-well plate at a path length of 5.8 mm for a 200 µL reaction volume at room temperature. The catalytic parameters were achieved by fitting the data to the Michaelis–Menten equation with the Graph-Pad Prism 5.0 software. If v_{max} was not reached, the catalytic efficiency was determined by fitting the linear part of Michaelis–Menten plot to a linear regression by using Graph-Pad Prism 5.0. Measurements were performed in at least triplicate.

Lactonase assay: AHL lactonolysis, consisting of the opening of the lactone ring, generated a proton and led to acidification of the media. This property allowed the kinetic characterization of the lactonases by using a pH indicator assay, as previously described.[13,14,24] To perform the experiment, enzyme (5 µL) was added to a solution containing substrates (10 µL) at various concentrations and lactonase buffer (185 µL; 2.5 mM Bicine pH 8.3, 150 mM NaCl, 0.2 mM $CoCl_2$, 0.2 mM cresol purple, 0.5% DMSO). This assay was performed at 25 °C and the time course of lactone hydrolysis was recorded at $\lambda = 577$ nm. A wide range of lactones were tested: C4-AHL, C6-AHL, C8-AHL, C10-AHL, 3-oxo-C8-AHL, γ-butyrolactone, γ-heptalactone, γ-nonalactone, γ-decanolactone, δ-valerolactone, δ-octanolactone, δ-nonalactone, δ-decalactone, ε-caprolactone, ε-decalactone, and whiskey lactone. The kinetic parameters of GcL against C4-, C6-, C10-, and 3-oxo-C8-AHLs were previously published.[25]

Paraoxon assay: The catalytic activity against the organophosphate Paraoxon-ethyl was monitored through a colorimetric assay, as previously described.[14,51] The hydrolysis of Paraoxon-ethyl generated paranitrophenolate anions, which were yellow in color. The assay was performed by measuring the time course hydrolysis ($\varepsilon_{405\,nm} = 17\,000\ M^{-1}\,cm^{-1}$) of Paraoxon-ethyl in PTE buffer (50 mM HEPES pH 8.0, 150 mM NaCl, 0.2 mM CoCl2).

Biofilm inhibition assay: The bacterial strain *A. baumannii* ATCC 19606TM was used in this study. The biofilm inhibition assay was performed as previously described.[24] Briefly, biofilm assays were carried out in MOPS minimal medium. The 96-well round-bottomed plates (Costar) for biofilm assay with different concentrations of GcL were incubated at 37 °C with continuous agitation, and the biofilm was assayed 16 h post-inoculation by means of crystal violet staining. Cell density was estimated by measuring the absorbance at $\lambda = 600$ nm by using a plate reader (Synergy HTX multimode reader, BioTek). After drying the wells, 0.1% crystal violet solution (200 µL) was added. Crystal violet was solubilized with 30% acetone and aliquots (200 µL) from each well were transferred to fresh flat-bottomed 96-well plates (Fisherbrand, Fisher Scientific) to measure the absorbance at $\lambda = 550$ nm. Measurements were performed in six replicates.

Crystallization: GcL crystallization was performed as previously reported.[24] GcL samples, concentrated at 10 mg mL^{-1} were used to set up crystallization trays through the hanging-drop vapor-diffusion method. Diffraction-quality crystals were obtained by using 1–2.25 M ammonium sulfate and 0.1 M sodium acetate buffer (pH 4.0–5.5). Crystals appeared after 1 day at 292 K. Crystals were transferred and cryoprotected in a solution composed of the mother solution supplemented by 30% poly(ethylene glycol) (PEG) 400 and frozen in liquid nitrogen. Crystals of GcL in complex with C4 AHL and 3-oxo-C12 AHL were obtained through soaking. The crystals were transferred for 5 min to a solution containing the cryoprotectant (mother solution and 30% PEG 400) containing 20 mM lactone substrates.

Data collection, structure resolution, and refinement: XRD datasets were collected at 100 K by using synchrotron radiation on the 23-IDB and 23-IDD beamlines (Table 2) at the Advanced Photon Source (APS, Argonne, Illinois, USA). Diffraction data were collected at a wavelength of 1.033 Å and, depending on the data set, between 400 and 1250 images were collected, with 0.2 or 0.5° oscillation steps and an exposure time of 0.2 s (Table 2).

The integration and scaling of the XRD were performed by using the XDS package.[52] Data were processed in the *C*2 space group for the free and 3-oxo-C12AHL-bound enzyme, whereas the C4AHL-bound diffraction dataset belonged to the *R*3 space group. The molecular replacement was performed by using the structure of AiiB as a model (PDB ID: 2R2D; 44% sequence identity) in MOLREP.[53] Then, an automated model reconstruction of GcL was achieved by using Buccaneer[54] before manual improvement with the Coot program.[55] Cycles of refinement were performed by using REFMAC.[56] Final refinement statistics are shown in Table 2.

Anomalous X-ray scattering data: The chemical composition of metals bound to the active site of GcL were investigated through two anomalous X-ray data collections. Because we used $CoCl_2$ during the induction step, and because lactonases were previously reported to bind cobalt, we collected two sets of data at higher (7859 keV) and lower (7715 keV) energy than that of the Co K absorption edge. Data collection statistics are shown in Table S1.

Acknowledgements

This work was supported by the MnDrive Initiative, and BARD grant IS-4960-16 FR to M.E. This work was also prepared by M.E. using federal funds under award NA18OAR4170101 from Minnesota Sea Grant, National Sea Grant College Program, National Oceanic and Atmospheric Administration, U.S. Department of

Commerce. The statements, findings, conclusions, and recommendations are those of the authors and do not necessarily reflect the views of NOAA, the Sea Grant College Program or the U.S. Department of Commerce. This paper is journal reprint no. JR659 of the Minnesota Sea Grant College Program. We thank the Advanced Photon Source and beamline staff for access and support (23 ID-B and 23 ID-D).

Conflict of Interest

The authors declare no conflict of interest.

Keywords: bacterial signals · lactones · quorum quenching · quorum sensing · structure elucidation

[1] S. T. Rutherford, B. L. Bassler, *Cold Spring Harbor Perspect. Med.* **2012**, *2*, a012427.
[2] L. S. Chernin in *Bacteria in Agrobiology: Plant Nutrient Management* (Ed.: D. K. Maheshwari), Springer, Heidelberg, **2011**, pp. 209 – 236.
[3] L. Zhang, Y. Dong, *Mol. Microbiol.* **2004**, *53*, 1563 – 1571.
[4] B. LaSarre, M. J. Federle, *Microbiol. Mol. Biol. Rev.* **2013**, *77*, 73 – 111.
[5] N. Amara, B. P. Krom, G. F. Kaufmann, M. M. Meijler, *Chem. Rev.* **2010**, *110*, 195 – 208.
[6] S. Hraiech, J. Hiblot, J. Lafleur, H. Lepidi, L. Papazian, J. M. Rolain, D. Raoult, M. Elias, M. W. Silby, J. Bzdrenga, F. Bregeon, E. Chabrière, *PLoS One* **2014**, *9*, e107125.
[7] P. Gupta, S. Chhibber, K. Harjai, *Burns* **2015**, *41*, 153 – 162.
[8] Y. H. Dong, J. L. Xu, X. Z. Li, L. H. Zhang, *Proc. Natl. Acad. Sci. USA* **2000**, *97*, 3526 – 3531.
[9] Y.-H. Dong, L.-H. Wang, J.-L. Xu, H.-B. Zhang, X.-F. Zhang, L.-H. Zhang, *Nature* **2001**, *411*, 813 – 817.
[10] A. Guendouze, L. Plener, J. Bzdrenga, P. Jacquet, B. Rémy, M. Elias, J.-P. Lavigne, D. Daudé, E. Chabrière, *Front. Microbiol.* **2017**, *8*, 227.
[11] a) H.-W. Kim, H.-S. Oh, S.-R. Kim, K.-B. Lee, K.-M. Yeon, C.-H. Lee, S. Kim, J.-K. Lee, *Appl. Microbiol. Biotechnol.* **2013**, *97*, 4665 – 4675; b) S. Huang, C. Bergonzi, M. Schwab, M. Elias, R. E. Hicks, *PLoS One* **2019**, *14*, e0217059; c) M. Schwab, C. Bergonzi, J. Sakkos, C. Staley, Q. Zhang, M. J. Sadowsky, A. Aksan, M. Elias, *Front. Microbiol.* **2019**, *10*, 611.
[12] M. Elias, D. S. Tawfik, *J. Biol. Chem.* **2012**, *287*, 11 – 20.
[13] J. Hiblot, J. Bzdrenga, C. Champion, E. Chabrière, M. Elias, *Sci. Rep.* **2015**, *5*, 8372.
[14] J. Hiblot, G. Gotthard, M. Elias, E. Chabrière, *PLoS One* **2013**, *8*, e75272.
[15] J. Bzdrenga, J. Hiblot, G. Gotthard, C. Champion, M. Elias, E. Chabrière, *BMC Res. Notes* **2014**, *7*, 333.
[16] J. Hiblot, G. Gotthard, E. Chabrière, M. Elias, *PLoS One* **2012**, *7*, e47028.
[17] M. Harel, A. Aharoni, L. Gaidukov, B. Brumshtein, O. Khersonsky, R. Meged, H. Dvir, R. B. Ravelli, A. McCarthy, L. Toker, I. Silman, J. L. Sussman, D. S. Tawfik, *Nat. Struct. Mol. Biol.* **2004**, *11*, 412 – 419.
[18] M. Ben-David, M. Elias, J. J. Filippi, E. Dunach, I. Silman, J. L. Sussman, D. S. Tawfik, *J. Mol. Biol.* **2012**, *418*, 181 – 196.
[19] M. Ben-David, G. Wieczorek, M. Elias, I. Silman, J. L. Sussman, D. S. Tawfik, *J. Mol. Biol.* **2013**, *425*, 1028 – 1038.
[20] H. Bar-Rogovsky, A. Hugenmatter, D. S. Tawfik, *J. Biol. Chem.* **2013**, *288*, 23914 – 23927.
[21] D. Liu, P. W. Thomas, J. Momb, Q. Q. Hoang, G. A. Petsko, D. Ringe, W. Fast, *Biochemistry* **2007**, *46*, 11789 – 11799.
[22] R. Mascarenhas, P. W. Thomas, C.-X. Wu, B. P. Nocek, Q. Q. Hoang, D. Liu, W. Fast, *Biochemistry* **2015**, *54*, 4342 – 4353.
[23] K. Tang, Y. Su, G. Brackman, F. Cui, Y. Zhang, X. Shi, T. Coenye, X.-H. Zhang, *Appl. Environ. Microbiol.* **2015**, *81*, 774 – 782.
[24] C. Bergonzi, M. Schwab, T. Naik, D. Daudé, E. Chabrière, M. Elias, *Sci. Rep.* **2018**, *8*, 11262.
[25] C. Bergonzi, M. Schwab, M. Elias, *Acta Crystallogr. Sect. F Struct. Biol. Commun.* **2016**, *72*, 681 – 686.
[26] C. Bergonzi, M. Schwab, E. Chabrière, M. Elias, *Acta Crystallogr. Sect. F Struct. Biol. Commun.* **2017**, *73*, 476 – 480.
[27] J. Momb, C. Wang, D. Liu, P. W. Thomas, G. A. Petsko, H. Guo, D. Ringe, W. Fast, *Biochemistry* **2008**, *47*, 7715 – 7725.
[28] M. H. Kim, W. C. Choi, H. O. Kang, J. S. Lee, B. S. Kang, K. J. Kim, Z. S. Derewenda, T. K. Oh, C. H. Lee, J. K. Lee, *Proc. Natl. Acad. Sci. USA* **2005**, *102*, 17606 – 17611.
[29] D. Liu, B. W. Lepore, G. A. Petsko, P. W. Thomas, E. M. Stone, W. Fast, D. Ringe, *Proc. Natl. Acad. Sci. USA* **2005**, *102*, 11882 – 11887.
[30] I. M. AL-Kadmy, A. N. M. Ali, I. M. A. Salman, S. S. Khazaal, *New Microbes New Infect.* **2018**, *21*, 51 – 57.
[31] K.-G. Chan, H. J. Cheng, J. W. Chen, W.-F. Yin, Y. F. Ngeow, *Sci. World J.* **2014**, *2014*, 891041.
[32] R. C. Edgar, *Nucleic Acids Res.* **2004**, *32*, 1792 – 1797.
[33] P. Del Vecchio, M. Elias, L. Merone, G. Graziano, J. Dupuy, L. Mandrich, P. Carullo, B. Fournier, D. Rochu, M. Rossi, P. Masson, E. Chabrière, G. Manco, *Extremophiles* **2009**, *13*, 461 – 470.
[34] M. Elias, J. Dupuy, L. Merone, L. Mandrich, E. Porzio, S. Moniot, D. Rochu, C. Lecomte, M. Rossi, P. Masson, G. Manco, E. Chabrière, *J. Mol. Biol.* **2008**, *379*, 1017 – 1028.
[35] A. Ceniceros, L. Dijkhuizen, M. Petrusma, *Sci. Rep.* **2017**, *7*, 17743.
[36] E. Takano, *Curr. Opin. Microbiol.* **2006**, *9*, 287 – 294.
[37] J. Bzdrenga, D. Daudé, B. Rémy, P. Jacquet, L. Plener, M. Elias, E. Chabrière, *Chem.-Biol. Interact.* **2017**, *267*, 104 – 115.
[38] M. López, C. Mayer, L. Fernández-García, L. Blasco, A. Muras, F. M. Ruiz, G. Bou, A. Otero, M. Tomás, *PLoS One* **2017**, *12*, e0174454.
[39] J. Y. Chow, Y. Yang, S. B. Tay, K. L. Chua, W. S. Yew, *Antimicrob. Agents Chemother.* **2014**, *58*, 1802 – 1805.
[40] B. Michael, J. N. Smith, S. Swift, F. Heffron, B. M. Ahmer, *J. Bacteriol.* **2001**, *183*, 5733 – 5742.
[41] A. Trovato, F. Seno, M. Zanardo, S. Alberghini, A. Tondello, A. Squartini, *FEMS Microbiol. Lett.* **2014**, *352*, 198 – 203.
[42] L. Afriat-Jurnou, C. J. Jackson, D. S. Tawfik, *Biochemistry* **2012**, *51*, 6047 – 6055.
[43] Y. Zhang, G. Brackman, T. Coenye, *Peer J.* **2017**, *5*, e3251.
[44] P. Jacquet, J. Hiblot, D. Daudé, C. Bergonzi, G. Gotthard, N. Armstrong, E. Chabrière, M. Elias, *Sci. Rep.* **2017**, *7*, 16745.
[45] R. García-Contreras, M. Martínez-Vázquez, N. Velázquez Guadarrama, A. G. Villegas Pañeda, T. Hashimoto, T. Maeda, H. Quezada, T. K. Wood, *Pathogens Dis.* **2013**, *68*, 8 – 11.
[46] C. Vieille, G. J. Zeikus, *Microbiol. Mol. Biol. Rev.* **2001**, *65*, 1 – 43.
[47] C. F. Liu, D. Liu, J. Momb, P. W. Thomas, A. Lajoie, G. A. Petsko, W. Fast, D. Ringe, *Biochemistry* **2013**, *52*, 1603 – 1610.
[48] L. H. Wang, L. X. Weng, Y. H. Dong, L. H. Zhang, *J. Biol. Chem.* **2004**, *279*, 13645 – 13651.
[49] M. Safari, R. Amache, E. Esmaeilishirazifard, T. Keshavarz, *Appl. Microbiol. Biotechnol.* **2014**, *98*, 3401 – 3412.
[50] K. Tamura, D. Peterson, N. Peterson, G. Stecher, M. Nei, S. Kumar, *Mol. Biol. Evol.* **2011**, *28*, 2731 – 2739.
[51] J. Hiblot, G. Gotthard, E. Chabrière, M. Elias, *Sci. Rep.* **2012**, *2*, 779.
[52] W. Kabsch, *J. Appl. Crystallogr.* **1993**, *26*, 795 – 800.
[53] A. Vagin, A. Teplyakov, *Acta Crystallogr. Sect. D Biol. Crystallogr.* **2010**, *66*, 22 – 25.
[54] K. Cowtan, *Acta Crystallogr. Sect. D Biol. Crystallogr.* **2006**, *62*, 1002 – 1011.
[55] P. Emsley, K. Cowtan, *Acta Crystallogr. Sect. D Biol. Crystallogr.* **2004**, *60*, 2126 – 2132.
[56] G. N. Murshudov, A. A. Vagin, E. J. Dodson, *Acta Crystallogr. Sect. D Biol. Crystallogr.* **1997**, *53*, 240 – 255.

Manuscript received: January 11, 2019
Revised manuscript received: March 11, 2019
Accepted manuscript online: March 12, 2019
Version of record online: ■■ ▮▮, 0000

Welcome all! A new lactonase, capable of degrading acyl-homoserine lactones used for bacterial signaling, exhibits no measurable substrate preference. It is shown that the broad substrate specificity of this enzyme relates to the absence of structural determinants to accommodate the variable region of the signaling lactone molecules.

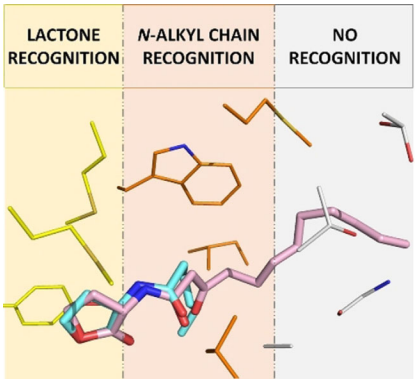

*C. Bergonzi, M. Schwab, T. Naik, M. Elias**

■■ – ■■

The Structural Determinants Accounting for the Broad Substrate Specificity of the Quorum Quenching Lactonase GcL